



# CATÓLICA

UNIVERSIDADE CATÓLICA PORTUGUESA | PORTO  
Escola Superior de Biotecnologia

***TEXTILE BASED 3D CONSTRUCTS TARGETTING  
FLAT BONE***

by

Maria Helena Moura Coimbra Soares

January 2017





# CATÓLICA

UNIVERSIDADE CATÓLICA PORTUGUESA | PORTO  
Escola Superior de Biotecnologia

## ***TEXTILE BASED 3D CONSTRUCTS TARGETING FLAT BONE***

Thesis presented to *Escola Superior de Biotecnologia* of the *Universidade Católica Portuguesa* to fulfill the requirements of Master of Science degree in Biomedical Engineering

by

Maria Helena Moura Coimbra Soares

Place: King's College London

Supervisor: Prof. Sanjukta Deb

Co-Supervisor: Prof. Ana Leite Oliveira

January 2017



*In loving memory of  
my grandfather,  
who I miss every day.  
He would be the most proud person with this victory  
started in London, his dream city .*



## Resumo

Ao longo dos anos, a engenharia de tecidos tem preenchido algumas lacunas e solucionado alguns problemas. Contudo, a engenharia de tecido ósseo ainda apresenta alguns problemas, mesmo com autoenxertos, considerados "*gold standard*" como morbidez do local dador, volume insuficiente e restrições na forma e tamanho do enxerto. Avanços recentes no desenvolvimento de biomaterias têm dado alternativas aos excertos ósseos, aumentando as opções para restaurar tanto a forma como a função do osso danificado. A engenharia de tecidos utilizando *scaffolds* é uma estratégia promissora para superar os obstáculos associados a excertos ósseos, melhorar a adesão celular, restaurando assim a forma e função do osso. *Scaffolds* tendo como base um têxtil têm vindo a ser utilizadas pois apresentam alta reprodutibilidade e maior controlo sobre o design e propriedades.

Um têxtil tridimensional (3D), feito de duas camadas de tecido de malha de trama da fibroína de seda espaçadas por um monofilamento de polietileno tereftalato (PET) foi modificado com fosfatos de cálcio, visando a criação de uma estrutura hierarquicamente montada esperando a optimização das suas propriedades mecânicas para crescimento osso chato. O compósito desenvolvido é caracterizado em termos de morfologia e propriedades mecânicas com impacto no comportamento ósseo, como resistência à flexão e resistência à tração. Três diferentes abordagens foram utilizadas para impregnar fosfatos de cálcio no têxtil, nomeadamente nitrato de cálcio tetra-hidratado e hidrogeno-fosfato de diamónio, brushite e hidroxiapatite em pó numa solução de 2% de alginato, sendo que hidroxiapatite (Hap)/alginato foi considerado o melhor devido à sua maior reprodutibilidade e facilidade de impregnação.

A análise FTIR feita comprovou a presença dos fosfatos de cálcio no interior do tecido.

O módulo de flexão é semelhante ao do osso esponjoso descrito na literatura.

Há um nível discrepância entre as características ideais dos substitutos ósseos que pode ser ultrapassado.









## **Abstract**

Over the years, tissue engineering has been consistently advancing with the prospects of new therapies targeting the regeneration of damage tissues. Bone tissue engineering is particularly challenging with autografts still being considered as the “gold standard” despite the related complications such as donor site morbidity, insufficient quantities, and restrictions in graft shape. Recent advances in the development of biomaterials have provided attractive alternatives to bone grafting expanding options for restoring the form and function of injured bone. Bone tissue engineering using scaffolds is a promising strategy in order to overcome bone grafts obstacles, by improving cell adhesion to scaffolds and restoring bone shape and function. Thus textile-based scaffolds have been recently proposed for bone tissue engineering since they present high reproducibility, precision and superior control over the design.

In this work, a three dimensional (3D) textile made of two weft-knitted silk fibroin fabric layers spaced by a monofilament of polyethylene terephthalate (PET) was modified with calcium phosphates aiming the creation of an osteoinductive, hierarchically patterned scaffold to meet the specific requirements of flat bone for craniofacial applications. Three different approaches were used, namely calcium nitrate tetrahydrate/diammonium hydrogen phosphate, brushite, and hydroxyapatite powder in a sodium alginate solution, to impregnate calcium phosphates in the 3D constructs. Among these, the Hap/alginate was proven to be the most effective.

The developed composites were characterized in terms of morphology, mechanical properties (flexural and tensile strength and Young's modulus) and Fourier transform infrared spectroscopy (FTIR). FTIR analysis allowed to confirm the presence of the calcium phosphates inside the fabric.

Despite the low strength, flexural modulus of selected composite was similar to the spongy bone flexural modulus described in the literature. There is often a great level of discrepancy between the ideal characteristics of bone substitutes and good and viable reproducibility that can be overcome.



## **Acknowledgements**

To King's College London, most importantly to my advisor, Dr. Sanjukta Deb, who gave guidance to be successful but yet freedom to explore on my own. She taught me how to question results and express ideas. Her support and advices helped me pass through some situations and finish this dissertation.

To Universidade Católica Portuguesa, most importantly, to my co-advisor, Dr<sup>a</sup> Ana Leite Oliveira, the first person who encouraged me to embrace the opportunity at King's College London. She provided the base material for my project and was always keen on helping and suggesting ideas.

To all those people working at the laboratory, who guided me on my first steps and along the way, this dissertation would not be the same without their help.

To those girls that were my nearest support during my stay at London, they made this journey an amazing one.

To the new friends that this dissertation brought to me I want to thank because they made everything easier and happier.

To my old friends that were there in all the moments that I needed them to be, good and bad ones, for being happy just because I was happy.

To my brother and sister who laugh at me when I most needed it making me see the (b)right side and keep me sane.

A very special "THANK YOU" to my parents who provided everything that I need during this time, they have been a constant source of love, guidance and support all these years.



# Contents

|   |             |
|---|-------------|
| <b>Resumo .....</b>   | <b>v</b>    |
| <b>Abstract .....</b>   | <b>vii</b>  |
| <b>Acknowledgements .....</b>   | <b>ix</b>   |
| <b>List of figures .....</b>  | <b>xiii</b> |
| <b>List of tables .....</b>   | <b>xv</b>   |
| <b>List of abbreviations .....</b>                                      | <b>xvii</b> |
| <b>1 - Introduction .....</b>   | <b>19</b>   |
| <b>1.1 Bone .....</b>   | <b>19</b>   |
| 1.1.1 Bone as nanocomposite.....  | 20          |
| 1.1.2 Bone cells .....  | 21          |
| 1.1.3 Mechanical properties .....                                       | 22          |
| 1.1.4 Bone remodelling.....   | 23          |
| <b>1.2 Bone tissue engineering .....</b>                                | <b>23</b>   |
| 1.2.1 Bone grafts .....   | 24          |
| 1.2.2 Scaffolds.....  | 24          |
| <b>1.3 Polymers .....</b>   | <b>27</b>   |
| <b>1.4 Bioceramics for bone tissue engineering.....</b>                 | <b>28</b>   |
| 1.4.1 Calcium phosphate (CaP) .....                                     | 28          |
| <b>1.5 Aim &amp; Hypothesis .....</b>                                   | <b>30</b>   |
| <b>2 - Materials and methods.....</b>                                   | <b>31</b>   |
| <b>2.1 Reagents.....</b>  | <b>31</b>   |
| <b>2.2 Production of the textile-based scaffolds .....</b>              | <b>31</b>   |
| <b>2.3 Degumming of the 3D textile constructs .....</b>                 | <b>32</b>   |
| <b>2.4 Impregnation of the 3D Textile.....</b>                          | <b>32</b>   |
| 2.4.1 Calcium nitrate tetra hydrate/Diammonium hydrogen phosphate ..... | 32          |
| 2.4.2 Brushite .....  | 32          |
| 2.4.3 Hydroxyapatite/2% Alginate.....                                   | 33          |

|  |           |
|--|-----------|
| <b>2.5 Characterization .....</b>  | <b>33</b> |
| 2.5.1 Contact angle measurements and plasma treatment.....                 | 33        |
| 2.5.2 Fourier Transform Infrared Spectroscopy (FTIR) .....                 | 34        |
| 2.5.3 Mechanical tests .....   | 34        |
| <b>2.6 - Statistical analysis.....</b>                                     | <b>35</b> |
| <b>3 - Results and Discussion .....</b>                                    | <b>37</b> |
| <b>3.1 Macroscopic morphology of the textile scaffold composites .....</b> | <b>37</b> |
| <b>3.2 Contact angle measurements .....</b>                                | <b>38</b> |
| <b>3.3 FTIR analysis .....</b>   | <b>40</b> |
| a) “Plain fabric” samples.....   | 40        |
| b) Brushite samples .....  | 41        |
| c) 2% alginate/HA samples .....  | 43        |
| <b>3.4 Mechanical Properties .....</b>                                     | <b>44</b> |
| a) Tensile tests.....  | 44        |
| b) Flexural tests .....  | 45        |
| <b>4 - Conclusion.....</b>   | <b>49</b> |
| <b>5 - Future work .....</b>   | <b>51</b> |
| <b>6 - References .....</b>  | <b>53</b> |



## List of figures

**Figure 1** – Hierarchical structural organization of bone.

**Figure 2** – Macroscopic image of flat bone.

**Figure 3** – The stress-distension curve and the load-deformation curve.

**Figure 4** – **a)** Full and **b)** Opened calcium nitrate tetrahydrate and diammonium hydrogen phosphate samples.

**Figure 5** – **a)** Paste method **b)** First soaked into liquid phase and **c)** First inserted with powder phase brushite samples.

**Figure 6** – **a)** Full and **b)** Opened brushite samples.

**Figure 7** – **a)** Full and **b)** Opened Ha/alginate samples.

**Figure 8** – Plain fabric sample FTIR spectrum.

**Figure 9** – Brushite sample FTIR spectrum.

**Figure 10** – 2% Alginate/HA sample FTIR spectrum.

**Figure 11** – Stress-strain curves from tensile test before and after 2% alginate/HA impregnation samples.

**Figure 12** – Stress-strain curves from flexural tests.







## List of tables

**Table 1** – Mechanical properties of cortical and cancellous bones.

**Table 2** – Advantages of scaffolds designed and fabricated via additive manufacturing.

**Table 3** – List of reagents.

**Table 4** – Mean contact angle and standard deviation before and after plasma treatment on dry and wet samples.

**Table 5** – FTIR spectral characteristics of plain fabric sample.

**Table 6** – FTIR spectral characteristics of brushite sample.

**Table 7** – FTIR spectral characteristics of 2% alginate/hydroxyapatite sample.

**Table 8** – Mean and standard deviation of maximum load, Young's Modulus and tensile stress of non-impregnated samples.

**Table 9** – Mean and standard deviation of maximum load, Young's Modulus and tensile stress of impregnated samples.

**Table 10** – Mean and standard deviation of maximum flexural load, flexural modulus and flexural stress.



## List of abbreviations

**ACP** – Amorphous Calcium Phosphate

**AM** – Additive manufacturing

**ATR** – Attenuated Total Reflectance

**Ca(H<sub>2</sub>PO<sub>4</sub>)<sub>2</sub>·H<sub>2</sub>O** – Monocalcium phosphate monohydrate

**Ca(NO<sub>3</sub>)<sub>2</sub>·4 H<sub>2</sub>O** – Calcium Nitrate Tetrahydrate

**Ca<sub>3</sub>(PO<sub>4</sub>)<sub>2</sub>** – Calcium phosphate

**CaP** – Calcium phosphates

**DSC** – Differential scanning calorimetry

**FTIR** – Fourier transform infrared spectroscopy

**H<sub>2</sub>O** – Water

**H<sub>3</sub>C<sub>6</sub>H<sub>5</sub>O<sub>7</sub>** – Citric acid

**L/P** – Liquid/powder ratio

**MCPM** – Monocalcium phosphate monohydrate

**Na<sub>2</sub>CO<sub>3</sub>** – Sodium carbonate

**NaOH** – Sodium hydroxide

**NH<sub>4</sub>H<sub>2</sub>PO<sub>4</sub>** – Di-ammonium hydrogen phosphate

**OCP** – Octacalcium phosphate

**RM** – Regenerative medicine

**SEM** – Scanning electron microscope

**SF** – Silk fibroin

**TCP** – Tricalcium phosphate

**TE** – Tissue Engineering

**β - Ca<sub>3</sub>(PO<sub>4</sub>)<sub>2</sub>** – β-tricalcium phosphate

**β - TCP** – β-tricalcium phosphate

**μ - CT** – Micro computed tomography









# 1 - Introduction

## 1.1 Bone

The human skeleton has a total of 213 bones, excluding sesamoid bones.<sup>(1)</sup>

Bone is made of two tissue types: slender fibres and lamellae connect to form a reticular structure - a spongy bone, also called cancellous bone or trabecular bone; and other with a high density texture - compact or cortical tissue- which incorporates increasing amounts of porous trabecular bone at the proximal and distal ends to optimise articular load transfer.<sup>(1)(2)</sup>

The relative amount of these two tissues varies in different bones according to the required strength or lightness needed, hence, there is a very heterogeneous composition depending on its function, it does not need to be exactly the same within the same bone. A deeper look of the compact tissue shows it to be highly porous structure, so the difference between it and the spongy bone is just the quantity of solid matter, the number and size of the spaces in each. These cavities in compact tissue are small and the solid matter between them is abundant-with a porosity of 3–12% and an average density of  $1.80 \text{ g}\cdot\text{cm}^{-3}$ . In cancellous bone, cavities are bigger and there is less solid matter .It has a porosity of 50–90% with an average trabecular spacing of around 1mm and an average density of approximately  $0.2 \text{ g}\cdot\text{cm}^{-3}$ .<sup>(2)(3)</sup>

Bone tissue has a hierarchical structural including macrostructure (cancellous and cortical bone), microstructure (Harversian systems, osteons, single trabeculae), sub-microstructure (lamellae), nanostructure (fibrillar collagen and embedded minerals) and sub-nanostructure (molecular structure of constituent elements, such as mineral, collagen, and non-collagenous organic proteins) (Figure 1).<sup>(2)</sup>

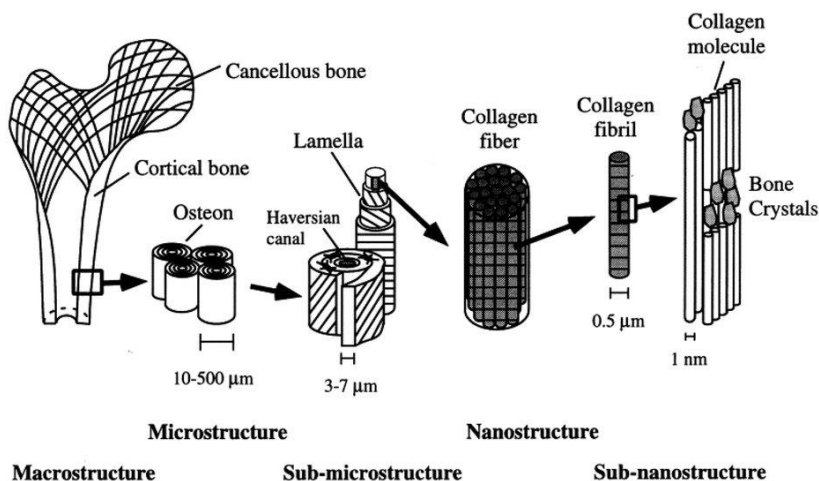


Figure 1 - Hierarchical structural organization of bone.<sup>(2)</sup>

There are four distinct categories of human body bones according to their form, size and shape. They differentiate, depending on their form, by long, flat, short and pneumatic bones.<sup>(4)</sup>

Flat bone, the target of this dissertation, has its central part made of spongy bone which is covered by two compact bone layers as can be seen on figure 2.<sup>(5)</sup>



**Figure 2** - Macroscopic image of flat bone.<sup>(6)</sup>

### **1.1.1 Bone as nanocomposite**

Bone tissue is a good example of a nanocomposite. Nanocomposites are defined as a heterogeneous combination of two or more kinds of components in which, at least one, is at the nanoscale, also known as a nanomaterial.<sup>(7)</sup> According to European Commission, since 2011, the definition of a nanomaterial is: “A natural, incidental or manufactured material containing particles, in an unbound state or as an aggregate and where, for 50% or more of the particles in the number size distribution, one or more external dimensions is in the size range of 1 nm–100 nm”.<sup>(8)</sup>

Composites are materials which combine two or more kinds of components. Its properties can be totally different from the homogenous materials that compose it.<sup>(9)</sup>

Bone tissue is composed of two major phases at the nanometer level: Organic (protein) and inorganic (mineral). These phases have some components that consist, in decreasing proportion in: Minerals, collagen, water, non-collagenous proteins, lipids, vascular elements, and cells.<sup>(10)</sup>

The mineral of bone is mainly composed of hydroxyapatite (HA) and the organic part of bone is mainly composed of collagen. Here, collagen acts as a structural framework in which plate-like tiny crystals of HA are embedded to strengthen the bone. Bone collagen has a typical fibrous structure, whose diameter varies from 100 to 2000 nm. Similarly, the HA in the bone mineral is in the form of nanocrystals, with dimensions of about 4 nm by 50 nm by 50 nm.<sup>(9)</sup>

The primary role of minerals is to provide toughness and rigidity to the bone, whereas collagen provides tensile strength and flexibility needed.<sup>(10)</sup> In other words, the function of collagen fibres is to provide strength in tension and resistance in bending whereas the apatite crystals embedded between the nanofibers will resist to compression.<sup>(11)(12)</sup>

### **1.1.2 Bone cells**

Bone is composed of four different cell types; osteoclasts, osteoblasts, bone lining cells and osteocytes.<sup>(13)</sup>

#### *Osteoclasts*

Osteoclasts are large multinucleated phagocytic cells that resorb the bone surface forming depressions known as Howship's lacunae. Dissolution of the inorganic fraction of the bone matrix is mediated by acidification of the bone surface by segregation of acids maintaining a low pH. The organic component is degraded by lysosomal proteolytic enzymes. These extensive exchanges between the cell and bone are effectively sealed off from the extracellular environment by the sealing zone. Osteoclasts migrate from bone marrow to a specific site and they also provide a long-term maintenance of blood calcium homeostasis.<sup>(13)</sup>

At sites of active resorption the organic and inorganic components of bone are endocytosed at the ruffled border, transcytosed through the cell in vesicles and liberated into the extracellular space via the plasma membrane domain.<sup>(13)</sup>

#### *Osteoblasts*

Osteoblasts are nucleus bone-forming cells with origin in stem cell from the bone marrow, which evidenced by the capacity of bone to regenerate itself both in vivo and in vitro by using cell populations. They act as seeding sites for hydroxyapatite crystal formation through localized enzymatic accumulation of calcium and phosphate and also promote mineralisation of the organic matrix.<sup>(13)</sup>

### *Bone Lining Cells*

Once osteoblasts have finished filling in a lacunae, bone surfaces are neither in the formative nor resorptive phase, the bone surface is completely lined by a layer of flattened and elongated old osteoblasts termed bone-lining cells. Lining cells cover the bone surface, protecting it from any osteoclast resorptive activity.<sup>(13)</sup>

### *Osteocytes*

Osteocytes are cells within the bone. They can have their origin in osteoblasts that turn into osteocytes while the new bone is being formed and then get surrounded by new bone. As they become more deeply situated they appear to be less active. The osteocytes live in lacunae where many fine canals (canaliculi) radiate from them in all directions which allows the diffusion of substances through the bone. As a result of their extensive distribution and interconnections, osteocytes can sense pressures or cracks in the bone and help to direct osteoclasts to the site where is necessary to dissolve the bone.<sup>(13)</sup>

### **1.1.3 Mechanical properties**

The mechanical properties of bone are conditioned by a few aspects such as bone composition (porosity, mineralisation) and structural organisation (trabecular or cortical bone architecture, collagen fibre orientation, fatigue damage). The resulting mechanical properties of the two types of bone tissue, namely, the cortical bone and cancellous bone, are shown in Table 1.

**Table 1-** Mechanical properties of cortical and cancellous bones.<sup>(2)</sup>

| <b>Property</b>                                | <b>Cortical Bone</b> | <b>Cancellous Bone</b> |
|--|----------------------|------------------------|
| <b>Compressive strength (MPa)</b>              | 100-230              | 2-12                   |
| <b>Flexural, Tensile strength (MPa)</b>        | 50-150               | 10-20                  |
| <b>Strain to failure (%)</b>                   | 1-3                  | 5-7                    |
| <b>Fracture toughness (MPam<sup>1/2</sup>)</b> | 2-12                 | -                      |
| <b>Young's modulus (GPa)</b>                   | 7-30                 | 0,5-0,05               |

### *Bone biomechanics*

Materials such as bones, whose stress-strain characteristics and resistance depend on the rate of deformation applied, are therefore, considered viscoelastic. This means that bone is not completely flexible or brittle, but a combination of these characteristics.<sup>(14)</sup> The cortical bone presents anisotropy,<sup>(15)</sup> which means that the mechanical properties are not equal in all directions and depend on the direction of load application. According to Wolff's law, its shape is given by the stress applied to it, which adapts dynamically through the structure and bone quantity. This law described possible bone changes, but not the mechanisms of these changes.

Bones will weaken if they are not subjected to adequate amounts of loading and weight bearing for sufficient periods of time, the amount and architecture of the bones can be improved by mechanical loading since bone reacts to changes by a process called remodelling.<sup>(14)</sup>

#### **1.1.4 Bone remodelling**

The shape and structure of bones are continuously modified and renovated .Bone remodeling involves the resorption of mineralized bone by osteoclasts followed by bone matrix formation by osteoblasts that afterwards become mineralized.<sup>(1)(3)</sup> The remodelling cycle consists in three phases: the resorption, during which osteoclasts digest old bone; reversal, during which mononuclear cells appear on bone superficies; and formation, when osteoblasts produce new bones until the resorbed bone is totally replaced. This bone remodelling allows the bone architecture adaptation to meet changing mechanical needs and it helps to repair microdamages in bone matrix preventing the accumulation of old bone.<sup>(2)</sup>

In the healthy young adult skeleton, the newly formed bone totally substitute the one removed on resorption phase. Later in the life, the amount of resorption slightly starts to be more than formation, resulting in a negative bone balance with aging.<sup>(14)</sup>

#### **1.2 Bone tissue engineering**

Functional bone tissue engineering using combinations of cells, scaffolds and bioactive factors is seen as a promising approach which can lead to a diversity of possibilities for bone regeneration and repair, in particular for the future development of hybrid materials which are able to exhibit suitable biomimetic and mechanical properties.<sup>(2)</sup>

### **1.2.1 Bone grafts**

There are different situations that lead to the need of a bone graft such as post-traumatic, degenerative, neoplastic or congenital/developmental damages/disease.<sup>(2)(9)(11)</sup> Despite the regenerative capacity of bone, 5–10% of all fractures tend to late union or progress towards a non-union. Both large traumatic bone defects and extensive loss of bone substance after tumour resection or revision surgery after still represent a major challenge in today's clinical practice.<sup>(2)</sup>

Bone grafts can have different origins which determine its designation:

Autografts, also called autogenous, are derived from the host animal; allografts are derived from the same species as the host animal; xenografts are derived from a species other than the host animal; or synthetic bone substitutes.<sup>(16)(17)</sup>

Autogenous bone is osteogenic (the cells within a donor graft produce new bone at the implantation site), osteoinductive (new bone is formed by mesenchymal stem cells from the surrounding tissue, which differentiate into osteoblasts), osteoconductive (vascularisation and new bone formation into the transplant) and highly biocompatible.<sup>(18)(19)</sup>

Defects are usually fixed by reconstructive surgery using an autogenous graft or allograft. However, both types of grafts have limitations which cannot be totally controlled. The major limitation of some allografts has been the immunogenic response to the foreign tissue of the graft. The tissue is often rejected by the body and is subject to an inflammatory reaction. Autogenous bone grafts are still considered the gold standard for bone regeneration although their limitations include donor site morbidity, insufficient volume, and restrictions in graft shape and contour.<sup>(20)(21)</sup>

In order to overcome these limitations, tissue engineering (TE) and regenerative medicine (RM) aim to: restore of tissue damage; improve cell adhesion to scaffolds to restore form bone form and function; improve proliferation of new-tissue formation inside the material without any inflammatory response.<sup>(22)</sup>

Great progresses have recently been made in the bone regeneration field, however, the ideal therapy was not yet found.

### **1.2.2 Scaffolds**

Scaffolds are three-dimensional structures which can both guide cell migration, proliferation and differentiation or serve as temporary mechanical support structure. Scaffolds need to fill some conditions. The best scaffold solution for bone repair should be



biocompatible, biodegradable, osteoconductive, osteoinductive, structurally similar to bone, and also needs to fill some other requirements like sufficient mechanical strength, adequate porosity (number and size) to allow tissue growth and waste and nutrients' transport.<sup>(23)(24)(25)</sup> Beside the material aspects, it should be easy to use, and cost-effective.<sup>(25)</sup>

### *Textile based scaffolds*

Tissue engineering (TE), is an area where textile technologies can have an important contribution since conventional techniques for scaffold fabrication like solvent casting, particulate leaching, gas foaming, fibre meshes and fibre bonding, phase separation, melt molding, emulsion freeze drying, solution casting or freeze drying<sup>(2)</sup> still present slow reproducibility. Also, conventional fabrication techniques available for scaffold production are not yet capable to fully meet the desired properties.<sup>(26)</sup>

Scaffolds processed by fibre-based technologies offer an extensive variety of morphological and geometric possibilities that can be tailored for each specific tissue-engineering application.<sup>(27)</sup> Therefore, textile-based technologies are considered as a potential route for the production of complex scaffolds for TE applications, as they can present superior control over the design, manufacturing precision and reproducibility.<sup>(26)(28)</sup> This technique has the advantages of a typical additive manufacturing technique (AM). Table 2 summarises the advantages of scaffolds designed and fabricated by AM techniques.

**Table 2** - Advantages of scaffolds designed and fabricated via additive manufacturing.<sup>(2)</sup>

| <b>Properties</b>     | <b>Advantages</b>  |
|-----------------------|--|
| <b>Variability</b>    | Higher variability of designing a targeted degradability and resorbility as well as improved biocompatibility.                         |
| <b>Formability</b>    | Can be processed into various shapes, volumes and microstructures.   |
| <b>Practicability</b> | Easily mass-produced or properties can be tailored for patient-specific applications (addressing the scheme of Personalised Medicine). |

|                           |  |
|---------------------------|--|
| <b>Controllability</b>    | Control over chemical and physically structural properties, crystallinity, hydrophobicity, degradation rate and mechanical properties (e.g through the alteration of surface chemistry).   |
| <b>Applicability</b>      | Allow exact engineering of matrix configuration, satisfying the biophysical limitations of mass transfer.  |
| <b>Flexibility</b>        | <p>Flexibility to alter the physical properties and potentially facilitate reproducibility and scale-up.</p> <p>Flexibility to manipulate the configuration of matrix to vary the surface area available for cell attachments, also to optimize the exposure of attached cells to nutrients and allow transport of waste products.</p> |
| <b>Design</b>             | The designs and fabrication of composite scaffolds which chemical environment surrounding a synthetic degradable polymer material be affected in a controlled fashion as the polymer by-products are neutralized by ceramic components.  |
| <b>Mass delivery</b>      | The potential to deliver continuously the nutrients and hormones that can be incorporated into the scaffold structure.   |
| <b>Surface properties</b> | The ration of surface area to mass can be altered or the porosity, pore size and pore size distribution of the differing configurations can be altered so as to increase or decrease the mechanical properties of the scaffold.  |

### 1.3 Polymers

Polymers are a class of synthetic materials characterised by its high processing versatility. Since polymer synthesis allows the direct control over chemical composition, it is extremely useful in bone substitution applications.<sup>(29)</sup> Polymer based scaffolds were firstly used in soft tissue engineering but, in last ten years, the development of high performance polymers and their combination with bioceramics has allowed the new generation of composites to act as scaffold materials for bone tissue engineering.<sup>(30)</sup>

When compared with natural polymers, hydrophilic synthetic polymers, like polyethylene terephthalate (PET), can easily be synthesized to fit the desired biological, physical, chemical and biomechanical properties of the tissue to be repaired, with specific structures and molecular weights offering improved control of the chemical composition and matrix architecture.<sup>(31)(32)</sup>

#### *Polyethylene terephthalate (PET) for bone regeneration*

Among all the polymeric materials that have been used as tissue engineering scaffolds, non-woven PET has been largely used in bone, cartilage and smooth muscle tissue engineering.<sup>(33)</sup> PET fibrous matrices possess stability, excellent mechanical strength, good biocompatibility and durability, a low elastic modulus, are relatively inert, biostable and have demonstrated a good behaviour when implanted in the human body.<sup>(32)</sup> Furthermore, its application as artificial ligaments, suture threads, weight-bearing materials in artificial joint prostheses and synthetic vascular prostheses further demonstrate its strength in tissue engineering.<sup>(33)(34)</sup> Lately, PET fibrous matrices have been used in bone scaffolds, cartilage and smooth muscle, osteosarcoma, cell proliferation, and the growth and differentiation of embryonic stem cells.<sup>(33)</sup> PET has a hydrophobic nature that can be changed by chemically treating it with sodium hydroxide or giving it a net positive charge using plasma electric discharge. This results in an increase in surface hydrophilicity resulting in enhanced cell attachment.<sup>(34)</sup>

#### *Silk*

Silk fibres are composed of two animal-based proteins: fibroin, which is a structural fibre embedded in the another protein, sericin, which is a protective protein.<sup>(35)</sup> Silk fibres have had increasing interest due to their impressive mechanical and biological properties. In recent years, silk-based composites have been extensively studied as promising

candidates in various application fields, such as tissue engineering,<sup>(36)</sup> technical textiles,<sup>(37)</sup> biosensors,<sup>(36)</sup> biomedical applications,<sup>(38)</sup> and drug delivery systems.<sup>(38)</sup>

### *Silk Fibroin*

Silk fibroin (SF) can be extracted from larvae cocoons of the species *Bombyx mori*. While preparing new SF-based biomaterials, there are important aspects to be considered like porosity and surface chemistry because these aspects affect cell behaviour, migration and proliferation.<sup>(36)</sup> Silk fibroin (SF) has been used as biomedical material due to its unique structure, biocompatibility, biodegradability, stability, and minimal inflammatory reaction, essential requirements for the design of scaffolds for bone regeneration, proved to be a good biomaterial for bone TE.<sup>(28)(35)(39)</sup>

## **1.4 Bioceramics for bone tissue engineering**

Bioceramics are mostly used in the repair of the skeletal system, including bone, joints and teeth, and to augment both hard and soft tissue. According to the types of bioceramics and host tissue interactions, they can be bioinert or bioactive. The bioactive ones may be resorbable or non-resorbable, and all these may be manufactured either in porous or dense bulk form, granules or coatings.<sup>(40)</sup>

The major bone substitutes are based on calcium phosphates, calcium sulphates and bioactive glasses, presented in the form of granules, blocks, pastes and putties.<sup>(41)</sup> Calcium phosphate ceramics (CPCs) have been widely used as biomaterials for the regeneration of bone tissue because of their capacity to induce osteoblastic differentiation.<sup>(42)</sup>

Despite the progress made in CPCs possessing, a range of surface chemistries and material properties with influence on cellular adhesion and differentiation is still unwell understood. Specifically, questions such as how the material properties contribute to osteoinductivity / osteoconductivity or why the osteoinduction level of certain CPCs may be higher than others.<sup>(41)</sup>

### **1.4.1 Calcium phosphate (CaP)**

Calcium phosphate (CaP) biomaterials simulate the main inorganic component of bone and form functional interfaces with the surrounding tissue, making it an interesting biomaterial.<sup>(41)</sup> Calcium phosphates are great candidates both for bone tissue engineering and bone substitute materials since they present excellent biocompatibility and are able to

integrate biologically with bone in the living body due to their similarity to poorly crystalline carbonated hydroxyapatite (HA), the main component of bone.<sup>(43)</sup>

The most commonly used CaPs include monocalcium phosphate monohydrate (MCMP), monocalcium phosphate anhydrous, dicalcium phosphate dihydrate, dicalcium phosphate anhydrous, octacalcium phosphate (OCP),  $\alpha$ - and  $\beta$ -tricalcium phosphate (TCP), amorphous CaP (ACP), calcium-deficient hydroxyapatite and HA.<sup>(44)</sup>

Nano-CaPs have great potential in bone repair and augmentation<sup>(41)</sup> as they exhibit better physicochemical and biological characteristics than conventional-sized CaPs, due to nano-CaPs being more similar to bone nanocrystals.<sup>(45)</sup>

### *Brushite*

Calcium phosphates cements (CPCs) typically consist of a solid and liquid phases which, mixed at specific molar ratio and pH, can yield cements that can be divided into two major types: apatite and brushite. When the pH of the cement paste is below 4.2 the product formed is dicalcium phosphate dehydrate, known as brushite.

Studies have indicated that acidic phosphates, like brushite, are osteoconductive, osteoinductive and resorb at a faster rate than HA.<sup>(43)</sup>

### *Hydroxyapatite*

Hydroxyapatite (Hap) has a similar chemical composition and structure to the mineral phase of human bones and hard tissues.<sup>(46)</sup> Because of its properties like biocompatibility, bioactivity, osteoconductivity, non-toxic, non-inflammatory and non-immunogenic response, it is a very good candidate for biomedical application.<sup>(47)</sup>

There are several ways to synthesize this mineral namely:

solid state reaction; using  $\text{CaHPO}_4 \cdot 2\text{H}_2\text{O}$  and  $\text{CaCO}_3$ .  $\text{CaHPO}_4 \cdot 2\text{H}_2\text{O}$  is ignited at 1100 °C to be converted in  $\text{Ca}_2\text{P}_2\text{O}_7$  and then mixed with  $\text{CaCO}_3$  in water. Finally, the solution is calcined at 1100 °C;

by precipitation, using calcium nitrate tetrahydrate ( $\text{Ca}(\text{NO}_3)_2 \cdot 4(\text{H}_2\text{O})$ ) and diammonium hydrogen phosphate ( $\text{NH}_4\text{H}_2\text{PO}_4$ );<sup>(48)</sup>

by precipitation using  $\text{Ca}(\text{OH})_2$  and  $\text{H}_3\text{PO}_4$ ;<sup>(48)</sup>

by precipitation of calcium ( $\text{Ca}^{2+}$ ) and phosphate ( $\text{PO}_4^{3-}$ ) ions, using calcium chloride and di-Sodium hydrogen phosphate ( $\text{Na}_2\text{HPO}_4$ ).<sup>(48)</sup>

## **1.5 Aim & Hypothesis**

This study intends the optimisation of mechanical properties from the fabric with calcium phosphates tailored to the requisites of bone.

## 2- Materials and methods

### 2.1 Reagents

The reagents used in this work are listed in the table below.

**Table 3** - List of reagents.

|  |  |                            |
|--|--|----------------------------|
| <b>Acrós Organics<br/>(USA)</b>            | Citric acid ,99%, pure, anhydrous  | $H_3C_6H_5O_7$             |
| <b>EDM Milipore<br/>(USA)</b>              | Sodium Hydroxyde pellets   | NaOH                       |
| <b>Fluka-<br/>BioChemika<br/>(Germany)</b> | Di-ammonium hydrogen phosphate   | $(NH_4)_2HPO_4$            |
|  | Alginic acid salt sodium from brown algae  | Sodium alginate            |
|  | Calcium Nitrate Tetrahydrate   | $Ca(NO_3)_2 \cdot 4 H_2O$  |
| <b>Sigma-Aldrich<br/>(Germany)</b>         | Hydroxyapatite nanopowder , < 200 nm particle size(BET), $\geq 97\%$ , Synthetic | $Ca_5(OH)(PO_4)_3$         |
|  | Moncalcium phosphate monobasic monohydrate                                       | $Ca(H_2PO_4)_2 \cdot H_2O$ |
|  | $\beta$ -Tricalcium phosphate purum p.a., $\geq 96.0\%$                          | $\beta - Ca_3(PO_4)_2$     |
| <b>Sigma-Aldrich<br/>(Portugal)</b>        | Sodium carbonate   | $Na_2CO_3$                 |

### 2.2 Production of the textile-based scaffolds

Silk derived from silkworm *Bombyx mori* was used in the form of yarns (supplied by the Portuguese Association of Parents and Friends of Mentally Disable Citizens (APPA-CDM, Portugal). Raw silk was processed into a 3D knitted spacer fabric by a weft-knitting technology (UP472T machine, Terrot, Germany), using silk yarns with for the outer layers and as a spacer yarn, a 100D/1F polyester monofilament (Putian Shuangyan Chemical Fiber Co., Ltd.) to create the Silk Fibroin- Polyethylene terephthalate (SF-PET) spacer fabric.

Textile scaffolds were first washed in a 0.15% (w/v) natural soap aqueous solution for 2 hours and then rinsed in distilled water to remove the impurities resulting from the manufacturing process. In this sense, SF-PET spacer fabrics underwent a subsequent purification process.

### **2.3 Degumming of the 3D textile constructs**

Saponification is a very common degumming process and was used to extract the sericin, which is known to present cytotoxicity,<sup>(28)</sup> from the all fibre regions within the textile matrices. Afterwards the silk structures underwent a subsequent degumming process of boiling for 60 min in a 0.03 M Na<sub>2</sub>CO<sub>3</sub> solution (Sigma-Aldrich, Portugal), and rinsing with boiling distilled water to ensure full extraction of sericin.

### **2.4 Impregnation of the 3D Textile**

#### **2.4.1 Calcium nitrate tetrahydrate / Diammonium hydrogen phosphate**

50 ml of 1 M Ca(NO<sub>3</sub>)<sub>2</sub>·4 H<sub>2</sub>O solution were prepared.

50 ml of 0,6 M (NH<sub>4</sub>)<sub>2</sub>HPO<sub>4</sub> solution were prepared.

Ca/P ratio was kept 1,67 to obtain the correct stoichiometry of hydroxyapatite (HA).

NaOH was added when necessary to both solutions to keep the pH above 10. The pH was measure with pH 211 Microprocessor pH Meter (HANNA instruments, Portugal).

The calcium nitrate solution was kept at 60 °C and continuously stirring while the ammonium phosphate solution was dropped into it in approximately 5 ml/min.

#### **2.4.2 Brushite**

Calcium phosphate cements consist in a mixture of liquid and solid phases that form a paste which solidifies.

Distilled water as liquid phase leads to a low seeding time of the formed paste which did not allow proper samples preparation so monosodium citrate solution was used as liquid phase, known to be a retardant, to increase the seeding time.<sup>(49)</sup>

To prepare the 0,5 M monosodium citrate solution were used 40 ml of H<sub>2</sub>O, 3,84 g of monosodium citrate and 0,8 g of sodium hydroxide.

Approximately 2,7 g of the powder phase were prepared using 1,5 g of β-Tricalcium phosphate and 1,2 g of Monocalcium phosphate monohydrate well mixed.



$\beta - \text{Ca}_3(\text{PO}_4)_2 + \text{Ca}(\text{H}_2\text{PO}_4)_2 \cdot \text{H}_2\text{O} \longrightarrow$  Powder phase

( $\beta$  - TCP + MCPM)

$\text{H}_3\text{C}_6\text{H}_5\text{O}_7 + \text{NaOH} + \text{H}_2\text{O} \longrightarrow$  Liquid phase

(Monosodium citrate)

Fabric samples were cut with 20 mm x 20 mm approximately. Three ways to precipitate the paste inside the fabric were tried, with a P/L ratio of 3:1.

- The powder and liquid phases were mixed until a paste was formed. Some samples were soaked in the paste and pressured by a glass rod, in other samples the paste was placed inside the fabric with a syringe;

-The fabric was immersed on the liquid phase and the solid phase was added after immersion;

- The fabric was impregnated with the powder and then soaked in the liquid phase.

All the samples were kept at 37 °C during 3 weeks.

### **2.4.3 Hydroxyapatite/2%Alginate**

200 ml of 2% sodium alginate solution was prepared by adding alginic acid salt sodium from brown algae to water to ensure a random distribution of hydroxyapatite inside the scaffold.

Hydroxyapatite powder was added in a P/L ratio of 1:10. The mixture was kept under continuously stirring until a homogenous solution was formed.

Several samples were cut with a scalpel with 20 mm x 20 mm approximately and soaked into the solution and impregnated under mechanical pressure to obtain a homogeneous concentration.

## **2.5 Characterization**

### **2.5.1 Contact angle measurements and plasma treatment**

The contact angle, performed to evaluate the wettability and efficacy of plasma treatment in brushite-treated samples, was measured on six samples (three dry and three wet) before and after treatment. Each sample was subjected to one measurement with 10  $\mu\text{l}$  of distilled water in vertical position and analysed with an image analyser.

Cold plasma treatment was applied during 10 seconds in each sample using a piezobrush PZ<sub>2</sub><sup>®</sup> by Relyon plasma (Germany).

### 2.5.2 Fourier Transform Infrared Spectroscopy (FTIR)

FTIR analysis provides data related with the chemical composition of the samples. Plain fabric, fabric with brushite and fabric with hydroxyapatite/alginate samples were opened in the middle to ensure the CPCs impregnation inside the fabric. Fourier transform infrared spectroscopy was made using a Spectrum One spectrophotometer (Perkin – Elmer), in the range of wavenumber from  $4000\text{ cm}^{-1}$  to  $650\text{ cm}^{-1}$  during 8 scans, with  $4\text{ cm}^{-1}$  resolution. The FTIR spectrum was normalized and smoothed to minimize possible interferences.

### 2.5.3 Mechanical tests

When a force is applied to a sealed object, it deforms. If the deformation is such that when removed the object returns to original position and conformation, is called "elastic deformation". When stress is applied until the point at which the object is no longer able to reverse its original form, is called "plastic deformation" and, finally, with the continuity of application of the load, the "fracture".

The angle of the curve identifies, in linear elastic portion of the region, the Young's modulus, while, in the plastic region, the total energy absorbed during the test and the final resistance as seen in figure 3.

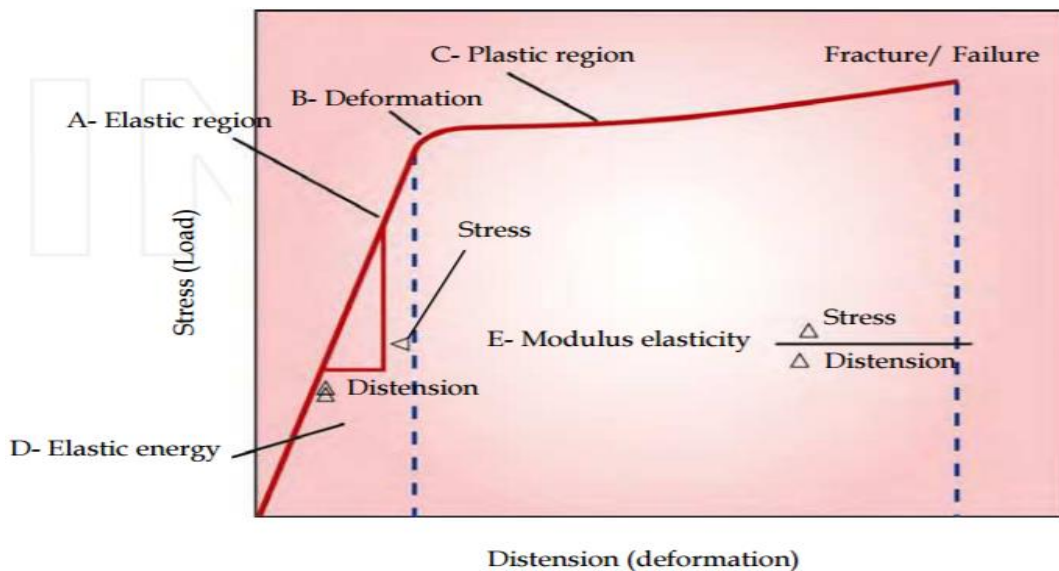


**Figure 3** - The stress-distension curve and the load-deformation curve.<sup>(50)</sup>

When the load is applied, there is an (A) initial elastic response that eventually reaches a (B) deformation point, getting into the (C) plastic response when the material is deformed permanently or is broken. The strength of the material is determined by the (D) energy or area

under the curve. (figure 3) The hardness of a material, called elasticity module is determined by the (E) inclination of the curve during the elastic response phase.

#### *Tensile tests*

Four samples of fabric without calcium phosphates and five Ha/alginate specimens were prepared with a dumbbell shape, with approximately 11,5 mm (maximum width) x 3,2 mm (thickness) and tested using an Instron 5596A (UK) at a speed of 7 mm/min.

In tensile tests, was considered the maximum load and calculated the Young's Modulus and tensile stress at the maximum load automatically.

#### *Flexural tests*

Six specimens were prepared with "trousers" shape with, approximately 12 mm width x 3,2 mm (thickness). A standard three-point flexural test was made using an Instron 5596A (UK) with a span length of 60 mm and a speed 5 mm/min.

In flexural tests, was considered the maximum flexure load and calculated the flexural modulus and the flexural stress at the maximum load automatically.

### **2.6 - Statistical analysis**

All the numerical results are presented as mean  $\pm$  standard deviation .Statistical analysis was performed using the *IBM SPSS Statistics 23* software. Nonparametric tests were used for all comparisons due low number of samples. The Mann-Whitney test was used to compare maximum load, Young's Modulus and tensile stress in samples without and with calcium phosphates. Regarding the contact angle measurements, the Wilcoxon test was used.

In both studies, was used a 95% confidence interval so the results were considered statistically significant when p-value < 5%.



### 3 - Results and Discussion

#### 3.1 Macroscopic morphology of the textile scaffold composites

The calcium phosphate cements (CPCs) impregnation using calcium nitrate tetrahydrate and diammonium hydrogen phosphate not fully effective. Beside the difficulty in keeping the pH above 10, a sample was opened to confirm the impregnation and there was no amount of precipitate (Figure 4).

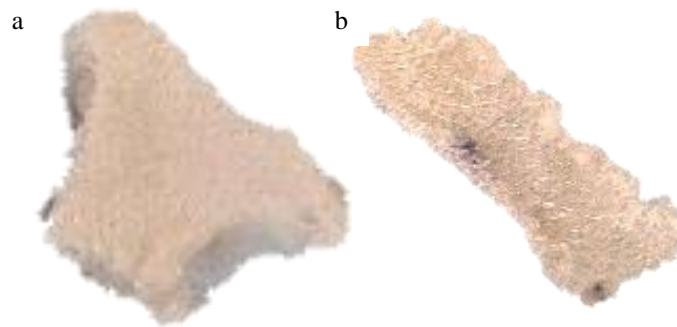


**Figure 4 - a)** Full and **b)** Opened samples after treatment calcium nitrate tetrahydrate and diammonium hydrogen phosphate.

As described in previous chapter (Materials and methods), three different ways to insert brushite inside the fabric were tried.

The method in which the paste was formed before impregnation (figure 5a) provided the best brushite formation and fabric impregnation. The paste could not be formed properly when the fabric was firstly soaked into the liquid phase (figure 5b) or the powder phased inserted before the soaking (figure 5c).

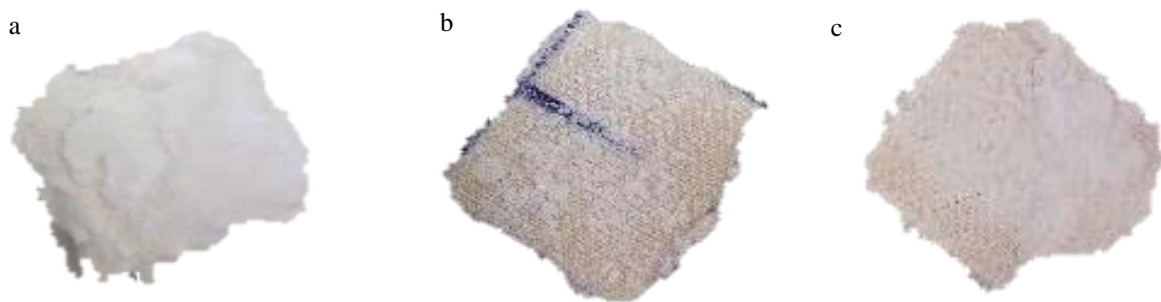


**Figure 5 - a)** Paste method **b)** First soaked into liquid phase and **c)** First inserted with powder phase brushite samples.

The paste method was the one adopted for brushite samples characterization. An opened sample was analysed and the impregnation inside the fabric was confirmed (figure 6b) by the white areas, both in brushite samples (figure 6) and Ha/alginate samples (figure 7).

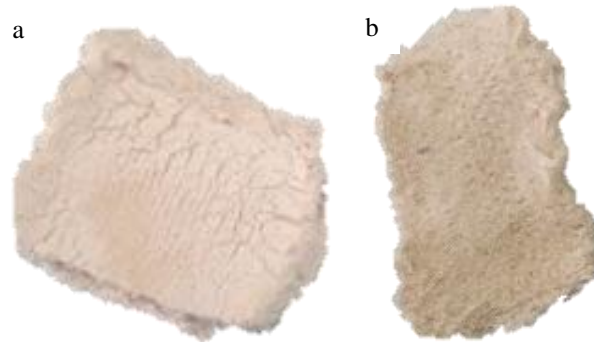


**Figure 6 - a) Full and b) Opened brushite samples.**

When compared to brushite, hydroxyapatite/alginate precipitation inside the textile was easier and that was confirmed by the higher amount of calcium phosphates in the interior of the fabric (Figure 7b).

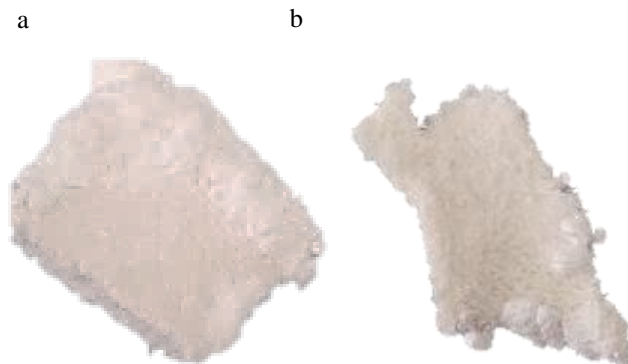


**Figure 7- a) Full and b) Opened Ha/alginate samples.**

The difficulty of cutting the textile with scissors/scalpel had influence on the borders of all samples.

### **3.2 Contact angle measurements**

Table 4 displays the mean contact angle from the dry and wet samples with their respective standard deviation both before and after the cold plasma treatment.

**Table 4** - Mean contact angle and standard deviation before and after plasma treatment on dry and wet samples.

|            | <b>Contact angle (°)</b>    |                            |
|------------|-----------------------------|----------------------------|
|            | <b>Before<br/>treatment</b> | <b>After<br/>treatment</b> |
| <b>Dry</b> | 114,12 ± 2,78               | 72,81 ± 2,58               |
| <b>Wet</b> | 83,20 ± 3,16                | 65,13 ± 3,58               |

Dry samples had a higher contact angle both before and after treatment. The major decrease of contact angle happens in the dry samples being that final contact angle is still lower in wet samples.

The chemical structure and the roughness of the surface changes, which can also change the wettability behaviour of the polymers since the cold plasma treatment creates a complex mixture of surface functionalities.<sup>(51)</sup>

The advantage of such plasma treatments is that the modification turns out to be restricted in the uppermost layers of the substrate, thus not affecting the overall desirable bulk properties.<sup>(52)</sup>

Traditional atmospheric pressure plasma devices are typically connected to high voltage or high power radio and microwave sources. This leads to unacceptable radiation contamination of the direct environment or to a high risk of electric shock. In addition, the necessary power supplies for these systems are technologically difficult and expensive.<sup>(53)</sup>

Piezobrush used to apply plasma treatment uses piezoelectric direct discharge, even not extensively tested on fabrics, is a small device that contraries the critical difficulty for the user to manage and uses a piezoelectric transformer as integral part of the plasma source so all high voltage problems of traditional atmospheric plasma sources can be avoided.<sup>(53)</sup>

As expected, the cold plasma treatment decreased the fabric wettability, however the difference has not statistical meaning ( $p > 0,05$ ) and the reduced angle was not sufficient to improve the brushite impregnation inside the fabric .

### 3.3 FTIR analysis

#### a) “Plain fabric” samples

Figure 8 displays the “plain fabric” FTIR spectrum. As expected, are visible the typical polyethylene terephthalate (PET) and silk fibroin (SF) bands. The main FTIR bands from the fabric before the impregnation are described in table 5.

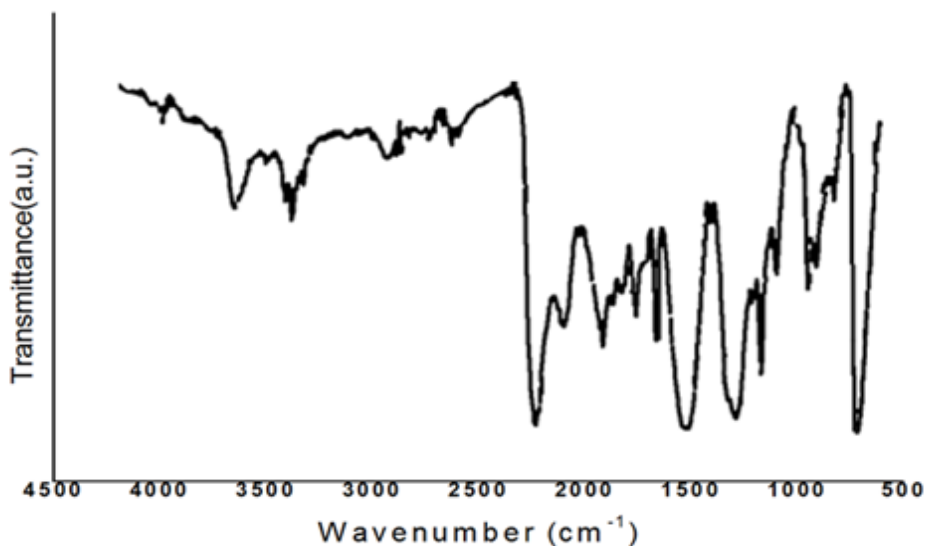


**Figure 8** – Plain fabric sample FTIR spectrum.

**Table 5** - FTIR spectral characteristics of fabric before impregnation.

| Wavenumber (cm <sup>-1</sup> ) | Assignment                  |
|--------------------------------|-----------------------------|
| 2800 - 4000                    | -OH Stretching              |
| 1713                           | C=O Stretching              |
| 1623                           | Amide I                     |
| 1520                           | Amide II                    |
| 1444                           | C-N Stretching              |
| 1408                           | C=C Stretching              |
| 1230                           | C-C-O Asymmetric Stretching |
| 1092                           | O-C-C Stretching            |
| 722                            | C-H Wagging                 |
| 694                            | Amide IV                    |



The intensity of bands between  $4000\text{ cm}^{-1}$  and  $2800\text{ cm}^{-1}$  vary in response to hydrogen bonds.

Around  $1713\text{ cm}^{-1}$  there is one band and assigned to  $\text{C}=\text{O}$  stretching vibration and at  $1408\text{ cm}^{-1}$ , there is a band assigned to  $\text{C}=\text{C}$  stretching vibration of the aromatic structure, both from PET fibres as the  $722\text{ cm}^{-1}$  band is related to the  $\text{C}-\text{H}$  wagging vibrations from the aromatic structures of PET fibres.<sup>(40)(54)(55)</sup> The molecular conformation of *B. mori* silk fibroin is characterized by  $\beta$ -sheet absorption bands around  $1630\text{ cm}^{-1}$ ,  $1530\text{ cm}^{-1}$  and  $1240\text{ cm}^{-1}$ , random coil conformation absorption bands at  $1650\text{ cm}^{-1}$  or  $1645\text{ cm}^{-1}$ ,  $1550\text{ cm}^{-1}$  and  $1230\text{ cm}^{-1}$ , and an  $\alpha$ -helix absorption band around  $1655\text{ cm}^{-1}$ .<sup>(56)</sup> Around  $1092\text{ cm}^{-1}$  there is a band corresponding to  $\text{O}-\text{C}-\text{C}$  stretching.

The band around  $1623\text{ cm}^{-1}$  related to amide I of Silk fibroin (SF)  $\beta$ -sheet structure,  $1520\text{ cm}^{-1}$  band is related to the amide II of SF  $\beta$ -sheet structure, bands at  $1444\text{ cm}^{-1}$  and  $1230\text{ cm}^{-1}$  and are given by  $\text{C}-\text{N}$  stretching, and last the band around  $694\text{ cm}^{-1}$  is due to amide IV, all from amide groups from silk protein,

All these characteristic absorbance bands indicate the existence of a hydrogen-bonded  $\text{NH}$  group.<sup>(57)</sup>

## b) Brushite samples

Figure 9 presents the FTIR spectrum obtained from samples before the impregnation with 2%alginate/HA and the main FTIR bands with the respective chemical group are described in table 6.

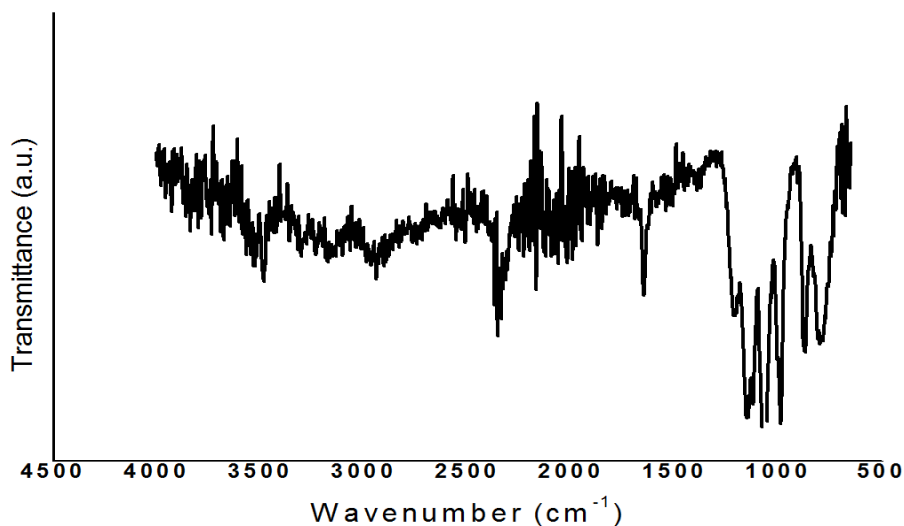


**Figure 9** – Brushite sample FTIR spectrum.

**Table 6** - FTIR spectral characteristics of brushite sample.

| <b>Wavenumber (cm<sup>-1</sup>)</b> | <b>Assignment</b>  |
|-------------------------------------|--------------------|
| 2368 - 3400                         | O-H Stretching     |
| 3481                                | -OH Stretching     |
| 1647                                | O-H Bond           |
| 1066                                | PO Stretching      |
| 985                                 | P-O (H) Stretching |
| 869                                 | P-O (H) Stretching |
| 793                                 | H-O-H Libration    |
|                                     | P-O (H) Stretching |

The 3481 cm<sup>-1</sup> band corresponds to the hydroxyl (-OH) vibrations of the water as the band between 2368- 3400 cm<sup>-1</sup> is due to O-H stretching vibration. Were expected another typical brushite two bands appearing as doublets close to 3530 cm<sup>-1</sup>, 3470 cm<sup>-1</sup> and 3270 cm<sup>-1</sup>, 3170 cm<sup>-1</sup> due to O-H vibration modes of the water that did not be identified strongly due the noise present at the spectrum. The bending mode due to the O-H bond from H<sub>2</sub>O was also detected as at 1647 cm<sup>-1</sup>.

At 1151 cm<sup>-1</sup> and 1066cm<sup>-1</sup> there are bands due to PO stretching vibrations as at 985cm<sup>-1</sup> and 869 cm<sup>-1</sup> bands are related to the P-O (H) stretching, from brushite phosphate group.

At 793cm<sup>-1</sup> is visible the band corresponding to H<sub>2</sub>O liberation and P-O (H) stretching.

There is no band associated to PET fibres, like the aromatic structure, which mean that FTIR sample was totally covered by brushite cement.

### c) 2%alginate/HA samples

Figure 10 presents the FTIR spectrum obtained from samples impregnated with 2%alginate/HA and the main bands with the respective chemical group are shown in table 7.

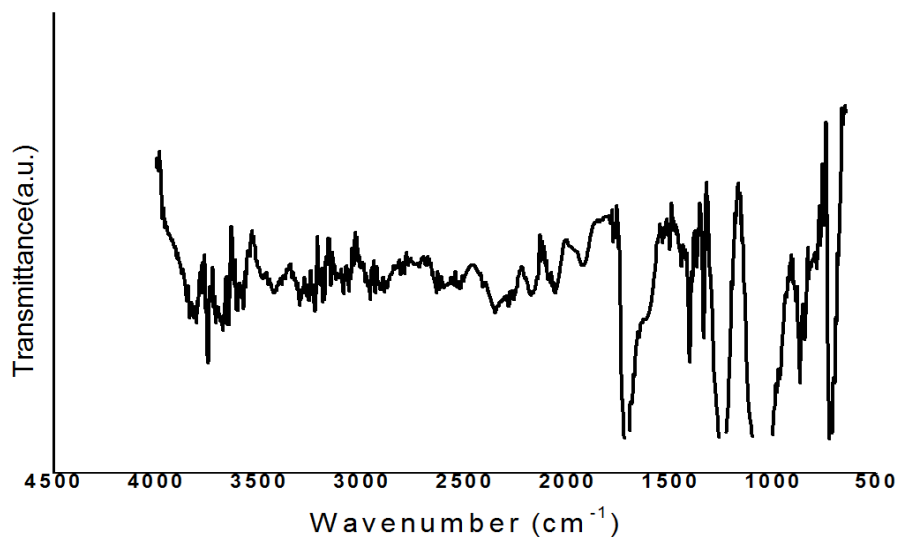


**Figure 10-** 2%Alginate/HA sample FTIR spectrum.

**Table 7-** FTIR spectral characteristics of 2%alginate/HA sample.

| Wavenumber (cm-1) | Assignment                  |
|-------------------|-----------------------------|
| 3572              | -OH Stretching              |
| 1713              | C=O Stretching              |
| 1408              | C-O-C Stretching            |
|                   | C=C Stretching              |
| 1259              | C-C-O Asymmetric stretching |
| 1092              | P-O Stretching              |
|                   | O-C-C Stretching            |
| 722               | C-H Wagging                 |

The wide absorption band between 3500 - 2400  $\text{cm}^{-1}$  is represents the hydroxyl groups.<sup>(58)</sup>

At 1713  $\text{cm}^{-1}$  there is a band corresponding to C=O stretching maybe from the protonation of carboxylate group.<sup>(59)</sup> The band from carbonyl group, typically around 1620  $\text{cm}^{-1}$  to alginate<sup>(60)</sup> shift to 1713  $\text{cm}^{-1}$  maybe because the proton was not displaced by a sodium ion.

The typical band around  $1634\text{ cm}^{-1}$  corresponding to hydroxyl vibrations from hydroxyapatite did not appear maybe due weak interaction between the alginate and hydroxyapatite powder.

The band around  $1408\text{ cm}^{-1}$  is attributed to the C-O-C stretching vibrations probably due to sodium alginate saccharide structure and C=C stretching vibration of benzene from PET. The  $1092\text{ cm}^{-1}$ , related to P-O vibration from  $\text{PO}_4^{3-}$  group and  $3572\text{ cm}^{-1}$ , from O-H stretch vibration, bands that are characteristic for hydroxyapatite spectrum, proving the fabric impregnation.<sup>(54)</sup>

The  $722\text{ cm}^{-1}$  band is related to the C-H wagging vibrations from the aromatic structures of PET fibres.<sup>(40)(54)(55)</sup>

In alginate/HA samples there are several bands related with PET fibres being that the tested sample was not fully covered with the paste.

### 3.4 Mechanical Properties

#### a) Tensile tests

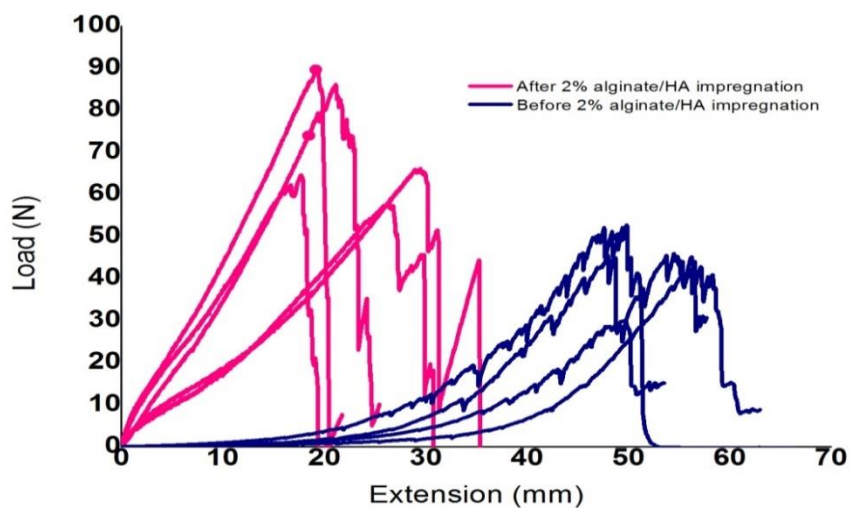


**Figure 11** - Stress-strain curves from tensile test before and after 2% alginate/HA impregnation samples.

**Table 8** – Mean and standard deviation of maximum load, Young’s Modulus and tensile stress of non-impregnated samples.

| Maximum Load<br>(N) | Young's Modulus<br>(MPa) | Tensile stress<br>(MPa) |
|---------------------|--------------------------|-------------------------|
| $46,798 \pm 4,188$  | $22,518 \pm 6,165$       | $3,615 \pm 0,830$       |

Before the impregnation, the fabric could take  $46,798 \pm 4,188$  N, corresponding to a tensile stress of  $3,615 \pm 0,830$  MPa. The Young's Modulus pre impregnation was  $22,518 \pm 6,165$  MPa.

**Table 9** - Mean and standard deviation of maximum load, Young's Modulus and tensile stress of impregnated samples.

| <b>Maximum Load<br/>(N)</b> | <b>Young's<br/>Modulus (MPa)</b> | <b>Tensile stress<br/>(MPa)</b> |
|-----------------------------|----------------------------------|---------------------------------|
| $73,140 \pm 14,070$         | $4,377 \pm 1,239$                | $1,974 \pm 0,367$               |

The Young's Modulus post-impregnation was  $4,377 \pm 1,239$  MPa, this is almost 10 times smaller than the minimum value in the literature (0,5GPa) for bone,<sup>(2)</sup> which means that the textile with the 2%alginate/HA as a low fracture resistance comparing to the natural bone.

The maximum load of  $73,140 \pm 14,070$  N, equals a tensile stress of  $1,974 \pm 0,367$  MPa, about 50 times smaller than the natural bone values.

As expected, the elastic modulus after the addition of calcium phosphates has decreased ( $p < 0.05$ ) since they turned the fabric in a less ductile material, beside the improved tensile stress, ( $p < 0.05$ ) this is still above the natural bone values.

#### **b) Flexural tests**

Among the prepared and subjected to a three-point bending test, only four were selected for analysis, the other ones were considered outliers because their obtained stress-strain curves were offset curves.

Although the most of the tested samples present similar flexural modulus values and graphs, the one that could be considered an outlier is the only presenting reasonable values and stress-strain graph (sample 1) so was considered for this study purposes and will be analysed and discussed, even if separately. The stress-strain curves can be seen in figure 13 and their values in table 7.

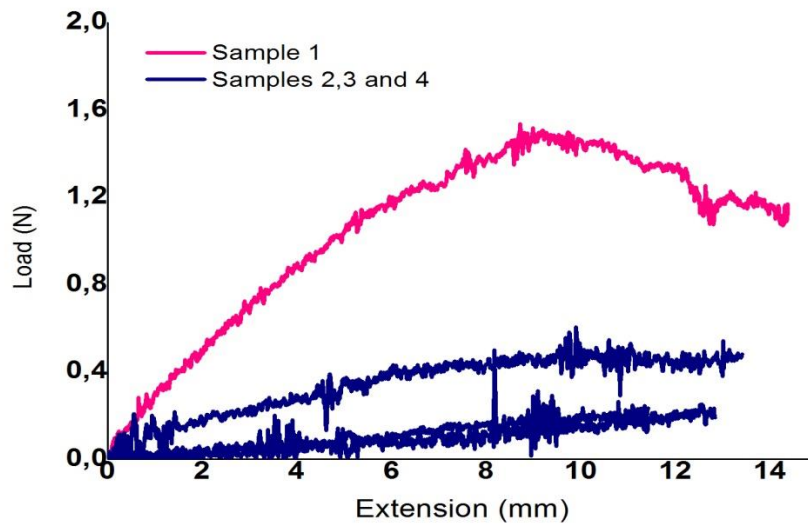


**Figure 12**-Stress-strain curves from flexural tests.

**Table 10** - Mean and standard deviation of maximum flexural load, flexural modulus and flexural stress.

|                 | <b>Maximum flexure<br/>load (N)</b> | <b>Modulus<br/>(Mpa)</b> | <b>Flexure stress<br/>(Mpa)</b> |
|-----------------|-------------------------------------|--------------------------|---------------------------------|
|                 | $0,473 \pm 0,147$                   | $0,757 \pm 0,084$        | $0,118 \pm 0,038$               |
| <b>Sample 1</b> | 1,537                               | 1105,628                 | 14,805                          |

Sample 1 had a flexural modulus of approximately 1,105 GPa which, according to Henkel, J. et al, <sup>(2)</sup> fits the cancellous bone modulus, and a flexure strength of 14,805 MPa. The three other samples present a mean flexural stress of  $0,118 \pm 0,038$  MPa and a flexural modulus of  $0,757 \pm 0,0841$  MPa only supporting  $0,475 \pm 0,147$  N of flexural load. The noise present in all the graphs comes probably from the dislocation of CPCs particles inside of the structure. As the samples are bending there is movement inside the fabric since the impregnated paste has porous and does not seed as unique cement but small particles.

The difference between samples can have several different reasons. Potential non-visible cracks induced by the human cutting can explain the low mechanical properties in samples 2, 3 and 4. The amount of paste within the fabric was not probably equivalent among the four samples, which can easily contribute for the variance of all the samples. Porosity presents an important role in both tensile and flexural stress, not only the number of pores but their sizes.<sup>(23)</sup> A scanning electron microscopy (SEM) analysis would be helpful to observe crack propagation and calcium phosphates distribution along the fabric.

Regardless of the fact that the mechanical properties of almost all the samples tested (excluding only flexural modulus from sample 1) are below the values described in the literature, their similarity is not a mandatory request as the composites formed by the fabric and 2%alginate/HA will be inserted inside the human body which can lead to changes in the morphology of the mineral crystals that could affect the homogeneity of the tissue and impact mechanical properties.<sup>(61)</sup>

Bone strength and toughness are positively correlated to bone mineral content, but when bone tissue becomes too highly mineralized, it tends to become brittle since tenacity (the capacity of absorption and keep the energy without breaking) is associated with low mineralization levels. A small increase of the mineral phase result in big increasing of resistance levels but reduces the tenacity<sup>(62)</sup>

The high flexibility of this new composite is a positive point as it allows an easier application by the doctor. Beyond that, once inside the human body, in vivo tissue responses will provide the optimization of the mechanical properties by promoting osseointegration.<sup>(59)</sup> The scaffold will be covered by the mineralized matrix formed by the cells which will naturally reinforce the composite therefore the mechanical properties will be improved.

Because tensile stress can be prescribed by cell geometry and tissue behaviour<sup>(61)</sup> is necessary a cell culture study to guarantee the proper mechanical properties of the scaffold in the living body.

The mechanical forces applied at bone are essential to the viability of bone cells. As bone cells are immobilized within a mineralized matrix, the transport of nutrients and oxygen is not made by diffusion. The mechanical forces applied to bone lead to deformations in the matrix which allow the fluid dislocation.<sup>(62)</sup>

There is a difficult balance between resistance and tenacity and bone cells nutrition and “stress break”.





## 4 - Conclusion

Bone tissue engineering should promote bone healing at the site of the defect and provide sufficient mechanical stability.

Textile-based scaffolds present a control over the design, manufacturing precision and reproducibility but the amount of calcium phosphate could not be exactly the same among all the samples. The aim of this study was improving the mechanical properties from a three dimensional (3D) textile made of two silk fibroin fabric layers spaced by a monofilament of polyethylene terephthalate (PET) by the integration of calcium phosphates. Three different hypotheses were firstly placed being that the alginate/HA was proven to be the best one, visually and by the FTIR analysis. The objective of this study was achieved as there were statistical significant differences in mechanical properties before and after impregnation.

Even that mechanical tests revealed values below the ones described in the literature for natural bone - 10 MPa for tensile and flexural test and 0,05 GPa for Young's modulus - in almost all the tested samples, (flexural modulus from sample 1 excluded), the scaffold will lately be inserted in the living body and thus populated by cells and mineralized matrix that can improved this mechanical properties so only further study can determinate if this new composite is viable.



## 5 - Future work

In the future, ideally, the fabric should be cut mechanically since it would be easier to have more accurate measurements, avoiding the sample cracks caused by human cut with scissors or scalpel, an important factor in mechanical tests.

It will be needed a way to guarantee a similar calcium phosphate (CaP) impregnation in the different samples and assure best porosity/strength to balance the biomechanical properties of the scaffold with its allowance to cell growth. A Micro Computed Tomography ( $\mu$ -CT) analyse, which was not possible due mechanical problems with the  $\mu$ -CT machine, will be helpful to visualize porous structure and possible air bubbles within the textile since it was soaked in the past and pressured,

There is often a great level of discrepancy between the clinical demands on a tissue engineering technique and the scientific realisation of such technique that will need to be checked and filled.



## 6 - References

- [1] Clarke, B. (2008). Normal bone anatomy and physiology. *Clinical Journal of the American Society of Nephrology*, 3(3), s131-s139. doi: 10.2215/CJN.04151206
- [2] Henkel, J., Woodruff, M. A., Devakara, D. R., Epari Steck, R., Glatt, V., Dickinson, I. C., Choong, P.F.M., Schuetz, M. A. & Hutmacher, D. W. (2013). Bone Regeneration Based on Tissue Engineering Conceptions - A 21st Century Perspective. *Bone Research* 1, 216–248 doi:10.4248/BR201303002
- [3] Hadjidakis, D.J. & Androulakis, I. I. (2006). Bone Remodeling. *ANNALS of the New York Academy Sciences*, 1092, 385-396. doi: 10.1196/annals.1365.035
- [4] Gray, H. (1918). *Anatomy of the human body 20<sup>th</sup>*. Lea & Febiger, Philadelphia
- [5] Sobotta, J. (1906). *Atlas and text-book of human anatomy Volume 1*. Philadelphia and London: W. B. Saunders Company.
- [6] Bostwick, P. & Florence, T. (2015). The Skeletal System. Presented at Darlington Technical College by Pearson Education, Inc.
- [7] Geckeler, K. & Nishide, H. (2009). *Advanced nanomaterials, Volume 1*. Germany: Wiley.
- [8] European Union, European Union for the Environment (2016). *Definition of a nanomaterial*. Retrieved from [http://ec.europa.eu/environment/chemicals/nanotech/faq/definition\\_en.htm](http://ec.europa.eu/environment/chemicals/nanotech/faq/definition_en.htm)
- [9] Sousa, H., Braga, M. & Sosnik, A. (2015). *Biomateriais aplicados ao desenvolvimento de sistemas terapêuticos avançados*. Coimbra: Imprensa da Universidade de Coimbra.
- [10] Murugan, R., Liao, S.S., Ramakrishna, S., Molnar, P., Huang, Z.M., Kotaki, M., Rao, K.P. & Hickman, J.J. (2009). Skeletal Regenerative Nanobiomaterials. Retrieved from <http://pminfonet.com/Murgan%202009b.pdf>
- [11] Murugan, R. & Ramakrishna, S. (2007). Nanoengineered biomimetic bone-building blocks. In G.A. Mansoori, T. F. George, L. Assoufid, & G. Zhang, (Eds.), *Molecular building blocks for nanotechnology* (pp. 301-352). New York: Springer.
- [12] Gardin, C., Ferroni, L., Favero, L., Stellini, E., Stomaci, D., Sivoletta, S., Bressan, E. & Zavan, B. (2012). Nanostructured biomaterials for tissue engineered bone tissue reconstruction. *International Journal of Molecular Sciences*, 13 (1), 737-57. doi: 10.3390/ijms13010737

- [13] Mohamed, A.M. (2008). An Overview of Bone Cells and their Regulating Factors of Differentiation. *The Malaysian Journal of Medical Sciences*, 5(1), 4–12.
- [14] Dalmolin, F., Pinto Filho, S.T.L., Cortes, A.M., Brun, M.V., Cauduro, C.R. & Schossler, J.E.W. (2013). Biomecânica óssea e ensaios biomecânicos: fundamentos teóricos. *Ciência Rural*, 43(9), 1675-1682. doi:10.1590/S0103-84782013000900022
- [15] Fan, Z., Swadener, J.G., Rho, J.Y., Roy, M.E. & Pharr, G.M. (2002). Anisotropic properties of human tibial cortical bone as measured by nanoindentation. *Journal of Orthopaedic Research*, 20, 806-810.
- [16] Zhang, J., Liu, W., Schnitzler, V., Tancret, F. & Bouler, J.M. (2014). Calcium phosphate cements for bone substitution: Chemistry, handling and mechanical properties. *Acta Biomateria* 10, 1035–1049.
- [17] Kumar, P., Vinitha, B. & Fathima, G. (2013). *Bone grafts in dentistry*. *Journal of Pharmacy & Bioallied Sciences*, 5 (1), s125-s127. doi: 10.4103/0975-7406.113312
- [18] Tadic, D. & Epple, A. (2004). A thorough physicochemical characterisation of 14 calcium phosphate-based bone substitution materials in comparison to natural bone. *Biomaterials*, 25(6), 987-994. doi: 10.1016/S0142-9612(03)00621-5
- [19] Greenwald, A.S., Boden, S.D., Goldberg, V.M., Khan, Y., Laurencin, C. T. & Rosier, R.N. (2001). Bone grafts substitutes: facts, fictions & applications. *The Journal of Bone and Joint Surgery*, 83(2), 98-103.
- [20] Tran, L., Krishnan, L., Priddy, L.B. & Guldborg, R.E. (2014). An effective alternative to autogenous bone grafts in critically sized defects. *Journal of Oral and Maxillofacial Surgery*, 72(9), e18-e19. doi: 10.1016/j.joms.2014.06.033
- [21] Pilia, M., Guda, T. & Appleford, M. (2013). Development of composite scaffolds for load-bearing segmental bone defects. *BioMed Research International*, 2013, 1-15. doi: 10.1155/2013/458253
- [22] Ribeiro, V.P., Morais, A., Correlo, V.M., Marques, A.P., Ribeiro, A.S., Silva, C.J., Durães, N.F., Bonifácio, G., Sousa, R.A., Oliveira, J.M., Reis, R.L. & Oliveira, A.L. (2015). *Complex 3D architectures based on knitting technologies for bone tissue engineering applications*. Paper presented at MedTex 2015\_International Conference on Medical Textiles and Healthcare Products, Poland.
- [23] Karageorgiou, V. & Kaplan, D. (2005). Porosity of 3D biomaterial scaffolds and osteogenesis. *Biomaterials*, 26(27), 5474-5491. doi:10.1016/j.biomaterials.2005.02.002
- [24] Jones, A.C., Arns, C.H., Huttmacher, D.W., Milthorpe, B.K., Sheppard, A.P. & Knackstedt, M.A. (2009). The correlation of pore morphology, interconnectivity and physical

properties of 3D Ceramic with bone ingrow. *Biomaterials*, 30, 1440-1451. doi:10.1016/j.biomaterials.2008.10.056

[25] Oryan, A., Alidadi, S., Moshiri, A. & Maffulli, N. (2014). Bone regenerative medicine: classic options, novel strategies, and future directions. *Journal of Orthopaedic Surgery and Research*, 9(18), 1-27. doi: 10.1186/1749-799X-9-18

[26] Ribeiro, V.P., Ribeiro, A.S., Silva, C.J., Durães, N.F., Bonifácio, G., Correlo, V.M., Marques, A.P., Sousa, R.A., Oliveira, A.L. & Reis, R.L. (2013). *Evaluation of Novel 3D Architectures Based on Knitting Technologies for Engineering Biological Tissues*. Paper presented at 2013 International Conference on Medical Textiles and Health Products (MedTex13), United States of America.

[27] Tuzlakoglu, K. & Reis, R.L. (2009). Biodegradable Polymeric Fiber Structures in Tissue Engineering. *Tissue Engineering*, 15(1), 17-27. doi:10.1089/ten.teb.2008.0016

[28] Ribeiro, V.P., Morais, A., Correlo, V.M., Marques, A.P., Ribeiro, A.S., Silva, C.J., Durães, N.F., Bonifácio, G., Sousa, R.A., Oliveira, J.M., Reis, R.L. & Oliveira, A.L. (2015, April). *Textile-based silk scaffolds for bone tissue engineering applications*. Poster session presented at 27<sup>th</sup> European Conference on Biomaterials ESB 2015, Poland.

[29] Laurecin, C.T., Ambrosio, A.M.A., Borden, M.D. & Cooper Jr., J.A. (1999). Tissue Engineering: Orthopedic Applications. *Annual Review of Biomedical Engineering*, 1, 19-45.

[30] Indrani, D.J., Budianto, E. & Purwasasmita, B.S. (2013). *Scaffolds of Hydroxyapatite and Alginate Composite for Tissue Engineering: Microstructure Analysis*. Paper presented at 3<sup>rd</sup> International Conference on Instrumentation, Communications, Information Technology, and Biomedical Engineering (ICIC-BME).

[31] Place, E.S., George, J.H., Williams, C.K. & Stevens, M.M. (2009). Synthetic polymer scaffolds for tissue engineering. *Chemical Society Reviews*, 38, 1139-1151. doi: 10.1039/B811392K

[32] Rojo, L., Vasquez, B. & Román, J. (2014). Biomaterials for scaffolds: synthetic polymers. In C. Migliaresi & A. Motta (Eds.), *Scaffolds for tissue engineering: biological design, materials, and fabrication* (pp.263-300). Singapore: Pan Stanford

[33] Lou, C., Li, M., Chen, W., Hu, J., Lu, C. & Lin, J. (2012). Preliminary Study of the Application of PET Knitted Fabrics in Artificial Bone Scaffold. *Applied Mechanics and Materials*, 184-185, 1501-1504. doi:10.4028/www.scientific.net/AMM.184-185.1501

[34] Basu, S. (2004). *Effects of three dimensional structure of tissue scaffolds on animal cell culture* (Doctoral dissertation thesis). Retrived from [https://etd.ohiolink.edu/rws\\_etd/document/get/osu1092689986/inline](https://etd.ohiolink.edu/rws_etd/document/get/osu1092689986/inline)

- [35] Oliveira, A.L., Sun, L., Kim, H.J., Hu, X., Rice, W., Kluge, J., Reis, R.L. & Kaplan, D.L. (2008). Aligned silk-based 3-D architectures for contact guidance in tissue engineering. *Acta Biomaterialia*, 8(4), 1530-42. doi: 10.1016/j.actbio.2011.12.015.
- [36] Altman, G.H., Diaz, F., Jakuba, C., Calabro, T., Horan, R.L., Chen, J., Lu, H., Richmond, J. & Kaplan, D.L. (2013). Silk-based biomaterials, *Biomaterials*, 24(3), 401-416. doi:10.1016/S0142-9612(02)00353-8
- [37] Li, Z., Ji, S., Wang, Y., Shen, X. & Liang, H. (2013). Silk fibroin-based scaffolds for tissue engineering. *Frontiers of Materials Science*, 7(3), 237-247. doi: 10.1007/s11706-013-0214-8
- [38] Rajkhowa, R., Tsuzuki, T. & Wang, X. (2010). Recent Innovations in Silk Biomaterials. *Journal of Fiber Bioengineering and Informatics*, 2(4), 202-213. doi:10.3993/jfbi03201001
- [39] Jiang, J., Wan, F., Yang, J., Hao, W., Wang, Y., Yao, J., Shao, Z., Zhang, P., Chen, J., Zhou, L. & Chen, S. (2014). Enhancement of osseointegration of polyethylene terephthalate artificial ligament by coating of silk fibroin and depositing of hydroxyapatite. *International Journal of Nanomedicine*, 9, 4569-4580. doi: 10.2147/IJN.S69137
- [40] Wang, P., Zhao, L., Liu, J., Weir, M., Zhou, X. & Xu, H. (2014). Bone tissue engineering via nanostructured calcium phosphate biomaterials and stem cells. *Bone Research*, 2, 1-13. doi: 10.1038/boneres.2014.17
- [41] Huang, J. & Best, S. M. (2007). Ceramic biomaterials. In A.R. Boccaccini, & J. Gough (Eds.), *Tissue Engineering Using Ceramics and Polymers* (pp.3-31). Cambridge: Woodhead Publishing Limited.
- [42] Deb, S. (2013). Calcium phosphate cements. In L. L. Hench (Eds.), *An introduction to bioceramics, second edition* (pp. 409-430). Singapore: Imperial College Press.
- [43] Dorozhkin, S.V. (2010). Nanosized and nanocrystalline calcium orthophosphates. *Acta Biomaterialia*, 6(3), 715-734. doi: 10.1016/j.actbio.2009.10.031
- [44] Chan, C.K., Kumar, T.S., Liao, S., Murugan, R., Ngiam, M. & Ramakrishnan, S. (2006). Biomimetic nanocomposites for bone graft applications. *Nanomedicine*, 1(2), 177-188. doi: 10.2217/17435889.1.2.177
- [45] Jin, H., Lee, C., Lee, W., Lee, J., Park, H. & Yoon, S. (2008). In situ formation of the Hydroxyapatite/chitosan-alginate composite scaffolds. *Materials Letters*, 62, 1630-1633. doi:10.1016/j.matlet.2007.09.043



- [46] Rajkumar, M., Meenakshisundaram, N. & Rajendran, V. (2011). Development of nanocomposites based on hydroxyapatite/sodium alginate: synthesis and characterisation. *Materials Characterization*, 62, 469-479. doi: 10.1016/j.matchar.2011.02.008
- [47] Leboucher, J.A. (n.d). Design and characterization of a scaffold for bone tissue engineering (Doctoral dissertation thesis). Retrived from <http://www.mate.tue.nl/mate/pdfs/2049.pdf>
- [48] Cama, G., Gharibi, B., Saif Sait, M., Knowles, J. C., Lagazzo, A., Romeed, S., Di Silvio, L. & Deb, S. (2012). A novel method of forming micro- and macroporous monetite cements. *Journal of Materials Chemistry B*, 1(7), 958-969. doi: 10.1039/C2TB00153E
- [49] Bankoff, A.D.P. (2012). Biomechanical Characteristics of the Bone. In T. Goswami (Eds.), *Human Musculoskeletal Biomechanics* (pp.61- 86). Croatia: InTech.
- [50] Rivera-Muñoz, E.M. (2011). Hydroxyapatite-Based Materials: Synthesis and Characterization. In R. Fazel-Rezai (Eds.), *Biomedical Engineering - Frontiers and Challenges* (pp. 75-98). Croatia: InTech. doi: 10.5772/19123
- [51] Bormashenko, E., Grynyov, R., Bormashenko, Y., & Drori, E. (2012). Cold Radiofrequency Plasma Treatment Modifies Wettability and Germination Speed of Plant Seeds. *Scientific Reports*, 2, 741. doi:10.1038/srep00741
- [52] Riccardi, C., Barni, R. & Esena, P. (2005). Plasma Treatment of Silk. *Solid State Phenomena*, 107, 125-128. doi:10.4028/www.scientific.net/SSP.107.125
- [53] Teschke, M. & Engemann, J. (2009). Piezoelectric Low Voltage Atmospheric Pressure Plasma Sources. *Contributions to Plasma Physics*, 49(9), 614 – 623 doi: 10.1002/ctpp.200910065
- [54] Strain, I.N., Wu, Q., Pourrahimi, A.M., Hedenqvist, M.S., Olsson, R.T. & Andersson, R.L. (2015). Electrospinning of recycled PET to generate tough mesomorphic fibre membranes for smoke filtration. *Journal of Materials Chemistry A*, 3, 1632-1640. doi:10.1039/C4TA06191H
- [55] Zhang, H., Li, L., Dai, F., Zhang, H., Ni, B., Zhou, W., Yang, X. & Wu, Y. N. (2012). Preparation and characterization of silk fibroin as a biomaterial with potential for drug delivery. *Journal of Translational Medicine*, 10, 117-126. doi: 10.1186/1479-5876-10-117
- [56] Tang, Y., Cao, C., Ma, X., Chen, C. & Zhu, H. (2006). Study on the preparation of collagen-modified silk fibroin films and their properties. *Biomedical Materials*, 1, 242–246. doi:10.1088/1748-6041/1/4/010

- [57] Parhi, P., Ramanam, A. & Ray, A.R. (2006). Preparation and characterization of alginate and hydroxyapatite-based biocomposite. *Journal of Applied Polymer Science*, 102(6), 5162- 6165. doi:10.1002/app.24706
- [58] Rehman, I. & Bonfield, W. (1997). Characterization of hydroxyapatite and carbonated apatite by photo acoustic FTIR spectroscopy. *Journal of Materials Science: Materials in Medicine*, 8(1), 1-4. doi:10.1023/A:1018570213546
- [59] Xu, J., Butler, I.S. & Gilson, D.F.R. (1999). FT-Raman and high-pressure infrared spectroscopic studies of dicalcium phosphate dihydrate ( $\text{CaHPO}_4 \cdot 2\text{H}_2\text{O}$ ) and anhydrous dicalcium phosphate ( $\text{CaHPO}_4$ ). *Spectrochimica Acta Part A: Molecular and Biomolecular Spectroscopy*, 55(14), 2801-2809. doi:10.1016/S1386-1425(99)00090-6
- [60] Burr, D.B. (2002). Bone material properties and mineral matrix contributions to fracture risk or age in women and men. *Journal of Musculoskeletal and Neuronal Interactions*, 2(3), 201-204.
- [61] Yuan, Y., Chesnutt, B.M., Wright, L., Haggard, W.O. & Bumgardner, J.D. (2008). Mechanical property, degradation rate, and bone cell growth of chitosan coated titanium influenced by degree of deacetylation of chitosan. *Journal of Biomedical Materials Research Part B: Applied Biomaterials*, 86(1), 245-252. doi: 10.1002/jbm.b.31012
- [62] Judas, F., Palma, P., Falacho, R.I. & Figueiredo, H. (2012). *Estrutura e Dinâmica do tecido ósseo*. Coimbra: Clínica Universitária de Ortopedia, HUC.